Published in final edited form as:
Nature. 2015 June 4; 522(7554): 106–110. doi:10.1038/nature14492.

The hypoxic cancer secretome induces pre-metastatic bone lesions through lysyl oxidase

Thomas R. Cox[1,2], **Robin M.H. Rumney**[3], **Erwin M. Schoof**[4], **Lara Perryman**[1], **Anette M. Høye**[1], **Ankita Agrawal**[3], **Demelza Bird**[2], **Norain Ab Latif**[3], **Hamish Forrest**[3], **Holly R. Evans**[3], **Iain D Huggins**[3], **Georgina Lang**[2], **Rune Linding**[1,4], **Alison Gartland**[#3,5], and **Janine T. Erler**[#1,2,5]

[1]Biotech Research and Innovation Centre (BRIC), University of Copenhagen (UCPH), Copenhagen, DK-2200, Denmark

[2]Hypoxia and Metastasis Team, Cancer Research UK Tumour Cell Signalling Unit, The Institute of Cancer Research, London SW3 6JB, UK

[3]The Mellanby Centre for Bone Research, The University of Sheffield, Sheffield S10 2RX, UK

[4]Cellular Signal Integration Group (C-SIG), Technical University of Denmark (DTU), Lyngby, DK-2800, Denmark

[#] These authors contributed equally to this work.

Abstract

Tumour metastasis is a complex process involving reciprocal interplay between cancer cells and host stroma at both primary and secondary sites, and is strongly influenced by microenvironmental factors such as hypoxia1. Tumour-secreted proteins play a crucial role in these interactions2–5 and present strategic therapeutic potential. Metastasis of breast cancer to the bone affects approximately 85% of patients with advanced disease and renders them largely untreatable6. Specifically, osteolytic bone lesions, where bone is destroyed, lead to debilitating skeletal complications and increased patient morbidity and mortality6,7. The molecular interactions governing the early events of osteolytic lesion formation are currently unclear. Here we show hypoxia to be specifically associated with bone relapse in ER-negative breast cancer patients. Global quantitative analysis of the hypoxic secretome identified Lysyl Oxidase (LOX) as significantly associated with bone-tropism and relapse. High expression of LOX in primary breast tumours or systemic delivery of LOX leads to osteolytic lesion formation whereas silencing or inhibition of LOX activity abrogates tumour-driven osteolytic lesion formation. We identify LOX as a novel regulator of NFATc1-driven osteoclastogenesis, independent of RANK Ligand, which disrupts normal bone homeostasis leading to the formation of focal pre-metastatic lesions. We show that these lesions subsequently provide a platform for circulating tumour cells to colonise

Correspondence and requests for materials should be addressed to janine.erler@bric.ku.dk and a.gartland@shef.ac.uk.

Author contributions J.T.E. and A.G. conceived the project, assisted by T.R.C. T.R.C., A.G. and J.T.E. designed the experiments. T.R.C., A.G. and R.M.H.R. performed the in vivo and in vitro experiments and analysed the data assisted by L.P., A.H., A.A., D.B., N.A.L., H.F., H.R.E., I.D.H. and G.L. T.R.C. and E.M.S. designed and performed the mass spectrometry and proteomics experiments and analysis, supervised by R.L. T.R.C. wrote and edited the paper, assisted by A.G., J.T.E., R.L. and R.M.H.R.

Author Information The authors declare no potential conflicts of interest.

Europe PMC Funders Author Manuscripts

and form bone metastases. Our study identifies a novel mechanism of regulation of bone homeostasis and metastasis, opening up opportunities for novel therapeutic intervention with important clinical implications.

Keywords

lysyl oxidase; breast cancer; hypoxia; pre-metastatic niche; bone; osteoclast; secretome; proteomics

Europe PMC Funders Author Manuscripts

Using a primary tumour hypoxic signature8, retrospective analysis of a cohort of lymph-node-negative breast cancer patients who received no systemic adjuvant therapy9 revealed a significant association with metastasis specifically within oestrogen receptor (ER)-negative (ER-) but not ER-positive (ER+) patients (Fig. 1a). Moreover, analysis of metastatic site showed significant association with bone metastases over lung, liver and brain (Fig. 1b and Extended Data Fig. 1a). We performed global differential quantitative mass-spectrometry-based proteomic analysis of the hypoxic secretome associated with osteotropism using the human ER- MDA-MB-231 parent and matched bone tropic (clone 1833) (MDA-BT)10 breast cancer cell lines (Fig. 1c). LOX was one of the most highly upregulated secreted proteins in MDA-BT cells (Fig. 1d, Supplementary Information 1 and Extended Data Fig. 1b–d). Querying the publically available data sets for the full panel of MDA-MB-231 clonal lines10, which exhibit differing levels of osteotropism, we found LOX was significantly associated with increasing osteotropism (Fig. 1e). LOX has previously been strongly implicated in cancer metastasis3,11–13, identifying it as an important candidate for further investigation.

Retrospective analysis of LOX in our patient cohort9 confirmed it is significantly associated with metastasis in ER- patients but not ER+ breast cancer patients (Extended Data Fig. 2a, b), consistent with previous reports13. Furthermore LOX is significantly associated with reported bone relapse across all patients and ER-, but not ER+, patients (Fig. 1f). Cox-regression analysis showed LOX is associated with increased hazard ratio in ER- patients for metastasis in general and bone relapse (Extended Data Fig. 2c). Receiver operating characteristic (ROC) analysis showed LOX is indicative of metastatic dissemination (including to the bone) in ER- but not ER+ breast cancer (Extended Data Fig. 3a). Importantly, our observations were confirmed in a second data set14 (Extended Data Fig. 3b). Our findings strongly implicate LOX in bone metastases in ER- breast cancer patients.

We further investigated our findings in the immune-competent 4T1-BALB/c syngeneic model of spontaneously metastasizing ER- breast cancer which expresses high levels of LOX3,13 (Extended Data Fig. 4a). The MDA-MB-231 lines are not suitable as a progression model since bone metastases do not occur from orthotopic implantation. Micro-computed tomography (micro-CT) analysis of bones from 4T1 tumour-bearing mice showed decreased trabecular and cortical bone volume, trabecular number and trabecular thickness, and increased focal osteolytic lesions over time (Fig. 2a–c and Extended Data Fig. 4b–e). Significant changes were detectable from 2 weeks after implantation when tumour hypoxia is a salient feature (Extended Data Fig. 4f). Bone marrow explants and quantitative PCR with reverse transcription (qRT–PCR) confirmed osteolytic lesion formation preceded the

arrival of tumour cells (Extended Data Fig. 4g–i). Strikingly, osteolytic lesion formation and cortical bone loss were also induced in a tumour-free model through injection of hypoxic tumour-conditioned media ('CM') (Fig. 2b, c)3. Our data show early osteolytic lesions are formed in the absence of tumour cells by hypoxia-induced tumour-secreted factors.

To determine LOX-dependency, mice were implanted with 4T1shLOX tumours, with decreased LOX expression and decreased LOX in sera (Extended Data Figs 4a and 5a). Micro-CT analysis revealed decreased osteolytic lesions in these mice (Fig. 2d, e), with no effect on primary tumour growth (Extended Data Fig. 5b). Immunological inhibition of LOX in 4T1 scrambled control (4T1scr) tumour-bearing mice with our antibody that binds specifically to LOX12 and blocks enzymatic function13, also decreased focal osteolytic lesion formation (Fig. 2f). Consistently, in tumour-free models, injection of 4T1shLOX CM generated fewer focal osteolytic lesions than 4T1scr CM (Fig. 2g).

We confirmed our findings in another, previously published human colorectal cancer model with manipulated LOX expression15. SW480 is a non-metastatic colorectal cancer cell line with low LOX expression, whose metastatic ability is increased by overexpression of wild-type LOX (+LOX) but not a catalytically inactive mutant (K320A) (+mutLOX)15. SW480+LOX CM injection showed increased frequency and size of osteolytic lesions compared with SW480+mutLOX or SW480+EV CMs (Fig. 2h and Extended Data Fig. 5c). While bone metastases in patients with colorectal cancer are rare, our data show that high levels of secreted active LOX drive focal osteolytic lesion formation in the bone independently of tumour presence across multiple cancer types. Injection of recombinant LOX (rLOX) into both immune-compromised nude and immune-competent BALB/c mice also led to the formation of focal osteolytic lesions (Fig. 2i) and increased circulating carboxy terminal telopeptide (CTX), a biomarker of bone turnover (Extended Data Fig. 5d). Our data clearly demonstrate tumour-secreted LOX as a mediator of osteolytic lesions.

Bone homeostasis is a balance between bone resorption by osteoclasts and bone formation by osteoblasts. This balance is typically disrupted in cancer metastasis. Addition of rLOX (in the absence of RANK ligand (RANKL)) to pre-osteoclast cultures was a highly effective stimulator of osteoclastogenesis, generating greater numbers of osteoclasts (Fig. 3a) with a higher resorptive capacity than RANKL-stimulated cultures (Fig. 3b, c). Enzyme-linked immunosorbent assays (ELISAs) for RANKL in rLOX-treated culture supernatants showed no RANKL, ruling out autocrine production of RANKL, and mass spectrometry analysis of rLOX preparations excluded the presence of contaminating effectors (Extended Data Fig. 6a, b). Our data show LOX can stimulate the generation of fully differentiated, active osteoclasts independently of RANKL.

Osteoclastogenesis is driven by the nuclear translocation of NFATc1, the master regulator of osteoclastogenesis16. Addition of rLOX (in the absence of RANKL) induced greater nuclear localization of NFATc1 than RANKL (Fig. 3d and Extended Data Fig. 6c), which was disrupted by treatment with our LOX-targeting antibody in a dose-dependent manner (Fig. 3e and Extended Data Fig. 6c). A by-product of LOX activity is the reactive oxygen species hydrogen peroxide (H_2O_2). Reactive oxygen species have previously been suggested to influence osteoclast differentiation and function17,18. Treatment of human pre-osteoclast

cultures with rLOX in the presence of catalase (which rapidly degrades H_2O_2) abrogated rLOX-driven NFATc1 nuclear localization in a dose-dependent manner (Fig. 3f). Our data identifies a novel, LOX-activity-dependent mechanism of *de novo* osteoclastogenesis which occurs independently of RANKL. Addition of rLOX to primary calvarial mouse osteoblasts decreased proliferation and led to an increase in terminal differentiation, which was attenuated by our LOX blocking antibody (Fig. 3g and Extended Data Fig. 6d). Similarly, high LOX 4T1scr CM decreased proliferation and increased differentiation of the human osteoblast SaOS-2 cell line (Extended Data Fig. 6e, f), which was attenuated by treatment with our LOX antibody. Our data show LOX leads to a loss of proliferative phenotype and increased terminal differentiation of osteoblasts.

Consistent with LOX tipping the balance of bone homeostasis in the favour of osteoclast resorption, quantification of osteoblasts and osteoclasts on the endocortical surface of tibiae from tumour-bearing mice showed decreased osteoblast and increased osteoclast number in 4T1scr tumour-bearing mice (Fig. 3h–j). Partial reversion was evident in mice treated with our LOX antibody and in mice bearing 4T1shLOX tumours (Fig. 3h–m and Extended Data Fig. 7a). Thus, tumour-secreted LOX is an important modulator of bone homeostasis. Treatment of tumour-bearing and CM-injected mice with clinically relevant concentrations of the bisphosphonate zoledronic acid abrogated focal osteolytic lesion formation (Fig. 4a–c) without affecting primary tumour growth (Extended Data Fig. 7b). Our data highlight the potential for therapeutic intervention of LOX-mediated osteoclast-driven pre-metastatic lesion formation in the bone.

The functional consequence of LOX-mediated pre-metastatic focal osteolytic lesion formation was tested by pre-conditioning BALB/c mice with either 4T1scr CM with or without LOX antibody, or 4T1shLOX CM to stimulate focal osteolytic lesion formation. 4T1 luciferase-expressing tumour cells (4T1Luc) were then injected intracardially. Bioluminescent IVIS imaging and micro-CT analysis revealed increased tumour burden in 4T1scr CM-conditioned mice compared with LOX antibody treated or 4T1shLOX CM-conditioned mice (Fig. 4d–f). A Pearson correlation coefficient showed a positive correlation between IVIS signal and lesion number (Extended Data Fig. 7c). Our data demonstrate that LOX-mediated pre-metastatic focal osteolytic lesions generate niches within the bone microenvironment that support colonization of circulating tumour cells and the formation of overt bone metastases. Treatment with bisphosphonate during 4T1scr CM conditioning of mice significantly reduced the ability of intracardially injected 4T1Luc cells to colonize the bone 1 week after injection and to develop bone metastases 5 weeks after injection (Fig. 4g, h). Thus, bisphosphonate treatment of patients with high-LOX-expressing tumours after surgery could prevent the establishment and growth of circulating tumour cells within the bone.

Pre-metastatic preparation of secondary sites to facilitate subsequent tumour cell colonization has been reported by us and others3,4,19 in several organs across multiple cancers; however, so far, the formation of pre-metastatic focal osteolytic lesions directly by tumour-secreted factors has not been described. We are the first to demonstrate, to our knowledge, that LOX activity modulates bone homeostasis, acting directly on osteoblasts and osteoclasts (Fig. 4i). Global bone loss before tumour cell arrival has been previously

linked to indirect effects of tumour-secreted factors through RANKL-dependent mechanisms20. We present a novel mechanism of deregulation of bone homeostasis independent of RANKL, yet acknowledge that other factors probably contribute to this inherently complex process. Interestingly, the post-translationally cleaved LOX propeptide, known for its opposing inhibitory effects to that of the mature LOX enzyme21, has been reported to modulate osteoblast behaviour through an intracellular mechanism inhibiting mineralization ability22. Yet embryonic day (E)18.5 $Lox^{-/-}$ mice exhibit markedly decreased mineral nodule formation and osteoblast differentiation23, supporting our data and suggesting context-dependent effects. LOX is reportedly expressed in osteoblasts and induced by TGF-β released during bone resorption24, which could further stimulate osteoclastogenesis leading to unbalanced coupling of bone homeostasis and focal osteolytic lesions. Since LOX-dependent pre-metastatic lesions form in the bone at the same time as those formed in the lungs and liver3, we believe that these osteolytic lesions are independent, forming simultaneously through unrelated mechanisms.

Our data suggest LOX may well be a useful marker for predicting the likelihood of metastases to the bone in ER- breast cancer patients and identifying these patients for adjuvant bisphosphonate treatment. Our data highlight that the dosing and administration of LOX inhibitors under development will be critical as genetic targeting yielded more potent effects than our antibody in this study, and earlier work has shown that treatment with the non-specific LOX inhibitor β-aminopropionitrile can reduce bone colonization in intracardiac models when administered at the time of inoculation25. In summary, our insight into the very early mechanisms of bone metastases before, and independent of tumour cell arrival, identifies a new step in bone metastasis and novel opportunities for therapeutic intervention.

Methods

For *in vivo* experiments, sample size was estimated to be eight mice per treatment group to ensure more than 80% power with 95% confidence, based on 25% practical difference and 15% coefficient of variation.

Patient data analysis

Evaluation of the expression of a previously published hypoxic signature8 and LOX with respect to metastasis and organ specific relapse was conducted using a published cohort of 344 primary breast cancers from lymph-node-negative patients who had not received systemic adjuvant therapy and with available gene expression data and site of relapse information. Details on patients and gene expression analysis can be found in ref. 9. P values were derived from a Mann–Whitney test and were two-tailed. An additional Kruskal–Wallis test between reported bone relapse, relapse elsewhere and no relapse patients with an additional contrast test wherein all pairwise groups were considered was conducted for LOX expression. Cox-regression using $\log_2$(LOX expression data) was used to estimate the hazard ratio in two analyses. One analysis used the no-relapse patients and the bone relapse patients, and the second analysis included all patients. An alternative second patient data

set14 reporting data on 295 lymph-node-negative patients who did not receive adjuvant therapy, with available site of relapse, was used to confirm our LOX-based findings.

In vitro culturing of tumour cells

Unless stated otherwise in the following sections, all cell lines were routinely cultured in DMEM with 100 U ml^{-1} penicillin and 100 mg ml^{-1} streptomycin, plus 10% FBS. For CM collection experiments, cells were transferred to serum-free DMEM without phenol red and incubated at either 21% oxygen (normoxia) or 1% oxygen (hypoxia) for 24 h in a Hypoxystation (Don Whitley Scientific). All CMs were filtered before use. For SILAC for mass spectrometry studies, tumour cells were grown in DMEM containing labelled isotopic amino acids, either light isotope (^{12}C-,^{14}N-arginine; ^{12}C-,^{14}N-lysine) (R0/K0) or heavy isotope (^{13}C-,^{15}N-arginine; ^{13}C-,^{15}N-lysine) (R10/K8) for five passages before incorporation was assessed. A minimum of 97–98% labelled arginine and lysine incorporation, with less than 1% proline conversion, was required for subsequent proteomics studies. The MDA-MB-231 BT cell line was obtained from J. Massague at the Memorial Sloan-Kettering Cancer Center. The 4T1 wild-type cell line was obtained from F. Miller at the University of Michigan. The SaOS-2 cell line was obtained from J. Gallagher at Liverpool University. The MDA-MB-231 parental cell line was obtained from the American Type Culture Collection (ATCC) (distributed by LGC Standards), where cell lines are authenticated on a regular basis. The 4T1Luc line was from SibTech. The 4T1 wild-type cell line was used to generate the 4T1shLOX line as previously published3. The SW480+EV, +LOX and +mutLOX cell lines were previously generated and authenticated using short tandem repeat analysis26. All cell lines were routinely tested for mycoplasma and tested negative for murine pathogens by IMPACT testing (IDEXX Laboratories).

Mass Spectrometry acquisition and secretome analysis

After collection, label-free and SILAC-labelled CMs were filtered and reduced in volume using 10 kDa molecular mass cut-off filters. The remaining protein was dissolved in 6 M urea, 2 M thiourea and 10 mM HEPES pH 8, after which exact protein amounts were determined using a Bradford assay. In SILAC-labelled repeats, the two SILAC labels (R10/K8 and R0/K0) were mixed 1:1. In label-free repeats, the samples were left unmixed as depicted in Fig. 1c, but equal amounts of starting material were used for processing. Proteins were reduced in 1 mM DTT (Sigma) for 45 min at room temperature (21°C), alkylated for 45 min using 5.5 mM chloroacetamide (Sigma), and digested with 1:50 (enzyme:protein ratio) of mass spectrometry (MS)-grade trypsin (Sigma) overnight at 37°C. Peptides were acidified with trifluoroacetic acid at a final concentration of 2%, and 5 mg of peptides were loaded onto a 50 cm C18 reverse-phase analytical column (Thermo EasySpray ES803) using an EASY nanoLC 1000. Peptides were eluted over a 4 h gradient ranging from 6 to 60% of 80% acetonitrile, 0.1% formic acid, and the Q-Exactive (Thermo Fisher Scientific) was run in a DD-MS2 top10 method. Full MS spectra were collected at a resolution of 70,000, with an AGC target of 3×10^6 or maximum injection time of 20 ms and a scan range of 300–1750 m/z. The MS2 spectra were obtained at a resolution of 17,500, with an AGC target value of 1×10^6 or maximum injection time of 60 ms. Dynamic exclusion was set to 45 s, and ions with a charge state <2 or unknown were excluded. MS performance was verified for consistency by running complex cell lysate quality control standards, and chromatography

was monitored to check for reproducibility. Raw data were processed using MaxQuant version 1.5 and Perseus version 1.4. Results were analysed using scripts written in-house in Python, and statistically tested for significance using the quantile function in the R statistical framework. To ensure high confidence identifications and quantification, a MaxQuant score of >50 and a minimum of two unique peptides per protein seen by tandem MS in all repeats were required. Initial analysis was undertaken using a label-free approach (two repeats) for global pairwise analyses, and data subsequently validated in a standard and reverse-label SILAC approach (two repeats). Identified intracellular contaminants were removed and secreted proteins retained by using the cellular compartment annotations in Ensembl and PantherDB, and Gene Ontology annotation enrichment for extracellular-associated terms. Raw mass spectrometry data along with in-house python scripts are available online at ProteomeXchange Consortium (http://proteomecentral.proteomexchange.org) with the data set identifier PXD000397.

Microarray data analysis of MDA-MB-231 cells

Previously published microarray data for parental and *in vivo* selected osteotropic subclones of the human MDA-MB-231 breast cancer line were retrieved (GEO accession number GSE2603). The subclones have previously been described and shown to be either weakly, mildly or strongly osteotropic10. All data sets were normalized and centred to the median of LOX probes.

In vivo models

Before the start of experiments, mice were randomly allocated into cages. Each mouse within the same cage received the same treatment. Cages were subsequently randomly allocated for treatment. Sample size was estimated to be eight mice per treatment group to ensure >80% power with 95% confidence, based on 25% practical difference and 15% coefficient of variation. For tumour-bearing studies, 2 x 10^5 4T1scr or 4T1shLOX or 4T1Luc cells were injected into the mammary fat pad of 8-week-old female BALB/c mice (Taconic). The tumour-free model has been previously described3, where 300 μl of tumour-cell CM is injected intraperitoneally daily into mice for 3 weeks. Rabbit anti-LOX (aLOX) antibody or rabbit IgG control treatments were administered intraperitoneally twice a week at 1 mg kg^{-1} 2 days after implantation. The LOX antibody (synthesized by OpenBiosystems) targets a conserved peptide sequence from the active site of human and mouse proteins, blocking function as previously described13, and has been shown not to bind other LOX family members12. For bisphosphonate studies, 0.6 mg kg^{-1} zoledronic acid was injected intraperitoneally twice a week. Primary tumour measurements were performed twice a week using calipers. All experiments were performed in accordance with UK Home Office regulations following UK Coordinating Committee for Cancer Research Guidelines for the Welfare and Use of Animals in Cancer Research, or under authorization and guidance from the Danish Inspectorate for Animal Experimentation. Cell line sources are stated above in ‘In vitro culturing of tumour cells’ and were tested negative for murine pathogens by IMPACT testing (IDEXX Laboratories). A second previously published human model of colorectal cancer with manipulated LOX expression15 was used to validate LOX-dependent findings. SW480 is a non-metastatic colorectal cancer cell line with low LOX expression, whose metastatic ability can be increased through expression of wild-type LOX

(SW480+LOX) but not a catalytically inactive mutant (K320A) (SW480+mutLOX)15. Eight-week-old female nude mice (Charles River) were injected daily with 300 μl SW480+EV (empty vector), SW480+LOX (full-length active LOX) or SW480+mutLOX (catalytically inactive mutant (K320A)) CM intraperitoneally for 3 weeks. Recombinant LOX (OriGene Technologies) in PBS was injected twice a week (25 μg kg^{-1}) intraperitoneally into 8-week-old female nude (Charles River) or BALB/c mice (Taconic) for 3 weeks. Exclusion criteria for data analysis were pre-established such that those mice terminated before defined experimental endpoints for ethical and/or licence reasons such as undue pain, suffering, distress and/or apparent lasting harm, or unexpected premature death, were not used for subsequent analysis. Values of n for all figures are displayed in accompanying legends.

Micro-CT imaging of tibia

Legs were removed from euthanized mice and fixed in either 4% paraformaldehyde solution or periodate–lysine–paraformaldehyde fixative. Fixed bones were dissected free of tissue and scanned on a micro-CT scanner (model 1172 Skyscan) at 50 kV with a 0.5 aluminium filter using a detection pixel size of 5 μm. The scanned images were reconstructed using Skyscan Recon software and analysed using Skyscan CT analysis software. A standard trabecular volume of interest was chosen starting 0.2 mm from the growth plate and included all trabeculae in a 1 mm^3 region of bone. Trabecular volume and number were assessed in this region. Total bone volume was also determined in a length of the bone from the top of the epiphysis to 3 mm below. Osteolytic lesions were measured through 360° of the bone on a three-dimensional model in a 3 mm length of cortical bone, starting at the growth plate. Holes smaller than 50 μm in diameter were excluded from the analysis as these represent normal physiological structures in bone. During analysis, investigators were blinded to specific treatment groups.

In vivo quantitation of osteoblast and osteoclast number

Tibiae were fixed in 4% paraformaldehyde solution, decalcified in 14.3% EDTA for 4 days at 37°C with daily changes of EDTA, then embedded in paraffin wax. Sections were cut (at 3 μm) using a Leica Microsystems Microtome and stained with tartrate-resistant acid phosphatase (TRAP) as described previously27. The numbers of osteoblasts and TRAP-positive osteoclasts were determined on a 3 mm length of endocortical surface starting 0.25 mm from the growth plate and viewed on a DMRB microscope (Leica Microsystems). All histomorphometric parameters were based on the report of the American Society for Bone and Mineral Research histomorphometry nomenclature28 and were obtained using the OsteoMeasure bone histomorphometry software (OsteoMetrics). During preparation and analysis of tibiae, investigators were blinded to specific treatment groups.

In vitro osteoclast and osteoblast models

Osteoclasts were generated on dentine disks from the $CD14^+$ fraction of human peripheral blood as previously described29. The $CD14^+$ cells were treated with 25 ng ml^{-1} recombinant M-CSF (-RANKL), plus either 30 ng ml^{-1} RANKL (+RANKL) or 150 ng ml^{-1} recombinant LOX (rLOX) (OriGene Technologies). The LOX antibody was added at 4 mg ml^{-1}. At the end of the culture period the cells were fixed and stained for TRAP. The number of TRAP-

positive osteoclasts and the amount of resorption were determined as previously described[30]. For NFATc1 nuclear localization, human peripheral blood monocytes were grown in standard osteoclastic conditions and the ability of LOX to induce nuclear localization of the transcription factor NFATc1 was measured at day 14 (mature, functional osteoclasts). For the role of LOX upon NFATc1 nuclear localization, cultures were treated for 24 h with rLOX; rLOX in the presence of the LOX antibody at 4 mg ml^{-1}; or LOX antibody alone at 4 mg ml^{-1}. To determine whether LOX-induced NFATc1 nuclear localization was mediated by reactive oxygen species, additional cultures were treated with 0, 50, 100, 150 and 200 U ml^{-1} catalase with and without rLOX (150 ng ml^{-1}). Primary murine calvarial osteoblasts were isolated from neonatal BALB/c mice as previously described27, and seeded into 96-well plates. To determine the effect of LOX on the differentiation and function of primary osteoblasts, cells were grown to confluence in normal medium (DMEM GlutaMAX with sodium pyruvate without phenol red, 100 U ml^{-1} penicillin and 100 mg ml^{-1} streptomycin, 10% FBS), and then switched to osteogenic medium (DMEM GlutaMAX with sodium pyruvate without phenol red (Life Technologies), 100 U ml^{-1} penicillin and 100 mg ml^{-1} streptomycin, 0.5% FBS and 50 mg ml^{-1} L-ascorbic acid (Sigma)) and treated with 10 nM dexamethasone (positive control), 150 ng ml^{-1} rLOX, or rLOX + LOX antibody. Cells were cultured in osteogenic medium for 3 weeks with the medium and treatments replaced every 2–3 days, and 5 mM inorganic phosphate added to all treatments 3 days before the end of the culture. Human osteoblast-like cells (SaOS-2), maintained as previously described[30], were treated with CM from 4T1 cells as previously described13 and the effect after 3 days on cell number was measured. SaOS-2 cells were also grown in osteogenic medium and the effect of the CM on the differentiation of these cells and their ability to mineralize was assessed after 7 days by quantification of alizarin red staining.

Quantification of mineralisation

Cells were rinsed in PBS and fixed in 100% ethanol overnight at 4°C. Nodules formed by osteoblasts were stained by alizarin red S. Briefly, cells were rinsed twice by PBS and incubated in 40 mM alizarin red S (pH 4.2) (Sigma) for 1 h at room temperature. Plates were washed with 95% ethanol on the shaker until the solution became clear; 10% cetylpyridinium chloride was then added to the wells and incubated at 55°C for 15 min, after which the absorbance was read at 550 nm.

NFATc1 staining and quantification

Cultures on coverslips were fixed with 4% paraformaldehyde for 15 min. Fixed cultures were rinsed three times between each subsequent step with 0.1% Tween in PBS and all incubations were at room temperature unless otherwise stated. Permeabilization was performed with 0.1% Triton X-100 in PBS for 10 min. Blocking was performed with 5% normal goat serum in PBS+0.1% Tween for 2 h. Mouse monoclonal antibody to NFATc1 (SC- 7294, Santa Cruz) and Mouse IgG_1 control were diluted 1:50 in 5% normal goat serum + 0.1% Tween and incubated at +4°C overnight. The secondary incubation was with Alexa Fluor 488 goat anti-mouse 1:300 in PBS for 1 h. The final incubation with rhodamine phalloidin 1:40 (R415, Invitrogen) and Hoechst 1:1,000 was for 20 min. Coverslips were mounted using ProLong Gold (Life Technologies). Images were captured with a Leica DMI 4000B fluorescence microscope at x20 objective with 0.70 aperture. NFATc1-positive nuclei

were counted with ImageJ. Each experiment was conducted with three independent donors. For each donor, each treatment group was set up in duplicate. For each duplicate, a minimum of 16 fields of view were quantified for nuclear NFATc1 signal.

Bioluminescent intravital imaging of bone colonisation

Adult female BALB/c mice (8 weeks old) were conditioned as described above. After 3 weeks of conditioning, mice were anaesthetized and 1 x 10^5 4T1Luc cells were injected intracardially into the left cardiac ventricle. Once a week, mice were injected with 120 mg kg^{-1} luciferin and metastatic dissemination of the cells was monitored using IVIS Lumina II (Caliper LifeSciences). Mice were killed by CO2 asphyxiation 3–5 weeks after tumour cell injection. Metastatic burden was quantified using Living Image software (Caliper Life Sciences) by measuring the luminescent signal from each leg; regions of interest are shown in Fig. 4. During analysis of IVIS data, investigators were blinded to specific treatment groups.

Immunoblotting

Immunoblotting for lysyl oxidase was as previously described3,13. Conditioned media and cellular lysates were prepared as previously described3,13. Primary LOX antibody (Open Biosystems) was used at 1:100 and β-actin (Abcam) at 1:10,000, with incubation overnight at 4°C. Species-specific biotinylated secondary antibodies were used at 1:25,000 and incubated for 1 h at room temperature, and visualization performed using ECL Plus (Amersham, GE Healthcare).

Immunohistochemistry for tumour hypoxia

Mice were injected intraperitoneally with pimonidazole (60 mg kg^{-1}) 1 h before culling. After excision, tumours were fixed in 4% PFA overnight before processing and embedding in paraffin according to standard histopathology techniques. Sections (4 μm) were cut and deparaffinized, rehydrated and stained with Hypoxyprobe (Hypoxyprobe) overnight after citrate-buffer-mediated antigen retrieval according to the manufacturer's guidelines. Hypoxyprobe binding was visualized with 3,3-diaminobenzidine before counterstaining with haematoxylin. Images were taken on a NanoZoomer slide scanner (Hamamatsu).

Explant cultures

The 4T1Luc line was implanted orthotopically as described above. Explant cultures of 4T1 tumour-bearing mice were generated at 1, 2, 3, 4 and 5 weeks after implant in the following ways. From primary tumour, small 5 mm^3 biopsies were taken and mechanically disaggregated to produce a single cell suspension. From lung, the left lobe was removed, washed and mechanically disaggregated to produce a single cell suspension. From bone, hindlimbs were separated at the joint and all extraneous tissue removed. Tibiae were opened at both end and bone marrow as well as tumour cells were flushed by syringe three times using PBS. From skin, a small 5 mm^2 punch of distant skin was mechanically disaggregated to produce a single cell suspension. Collected cells were washed and plated in standard serum containing media. Forty-eight hours after seeding, media were changed to remove non-adhered cells and 500 mg ml^{-1} Zeocin (the selective marker for the luciferase cassette)

was added for 2 weeks. D-Luciferin salt (Caliper Life Sciences) at a final concentration of 3 mg ml^{-1} was added just before bio-luminescent imaging using the IVIS Lumina II, and quantification of luminescent signal used Living Image software (Caliper Life Sciences).

Q-RTPCR

Total RNA was isolated from cells using TRizol (Invitrogen) and purified RNA treated with DNase I (New England Biolabs), both according to the manufacturer's instructions. Complementary DNA synthesis were performed using an M-MLV Reverse Transcriptase Kit (Invitrogen). qRT–PCR for β-actin and firefly luciferase was performed using a LightCycler 480 (Roche). Firefly luciferase was amplified using the primers 5'-CTCACTGAGACTACATCAGC-3' and 5'-TCCAGATCCACAACCTTCGC-3', and for β-actin 5'-GAGGCCCAGA GCAAGAGAGG-3' and 5'-TACATGGCTGGGGTGTTGAA-3'.

ELISA

ELISA plates were coated with sera from 4T1scr and 4T1shLOX tumour- bearing mice at 4°C overnight. Plates were blocked with 1% BSA at 37°C for 3 h. Our anti-LOX antibody was prepared in PBS containing 0.1% BSA, and 100 μl was added to wells for 2 h at room temperature. Binding of anti-LOX antibody to LOX protein was detected using horseradish peroxidase (HRP)-labelled secondary antibodies (1:10,000 dilution). The CTX-I ELISA (RatLaps) was used for quantitative determination of bone-related degradation products from CTX of type I collagen in mouse serum released by osteoclasts. All procedures were performed in accordance with the manufacturer's guidelines using sera from animals taken at time of cull. A sandwich ELISA for detecting human RANKL in the osteoclast medium was used according to the manufacturer's instructions (DuoSet, R&D Systems Europe). The sensitivity of the RANKL ELISA was 78.1–5,000 pg ml^{-1}.

Europe PMC Funders Author Manuscripts

Europe PMC Funders Author Manuscripts

Extended Data

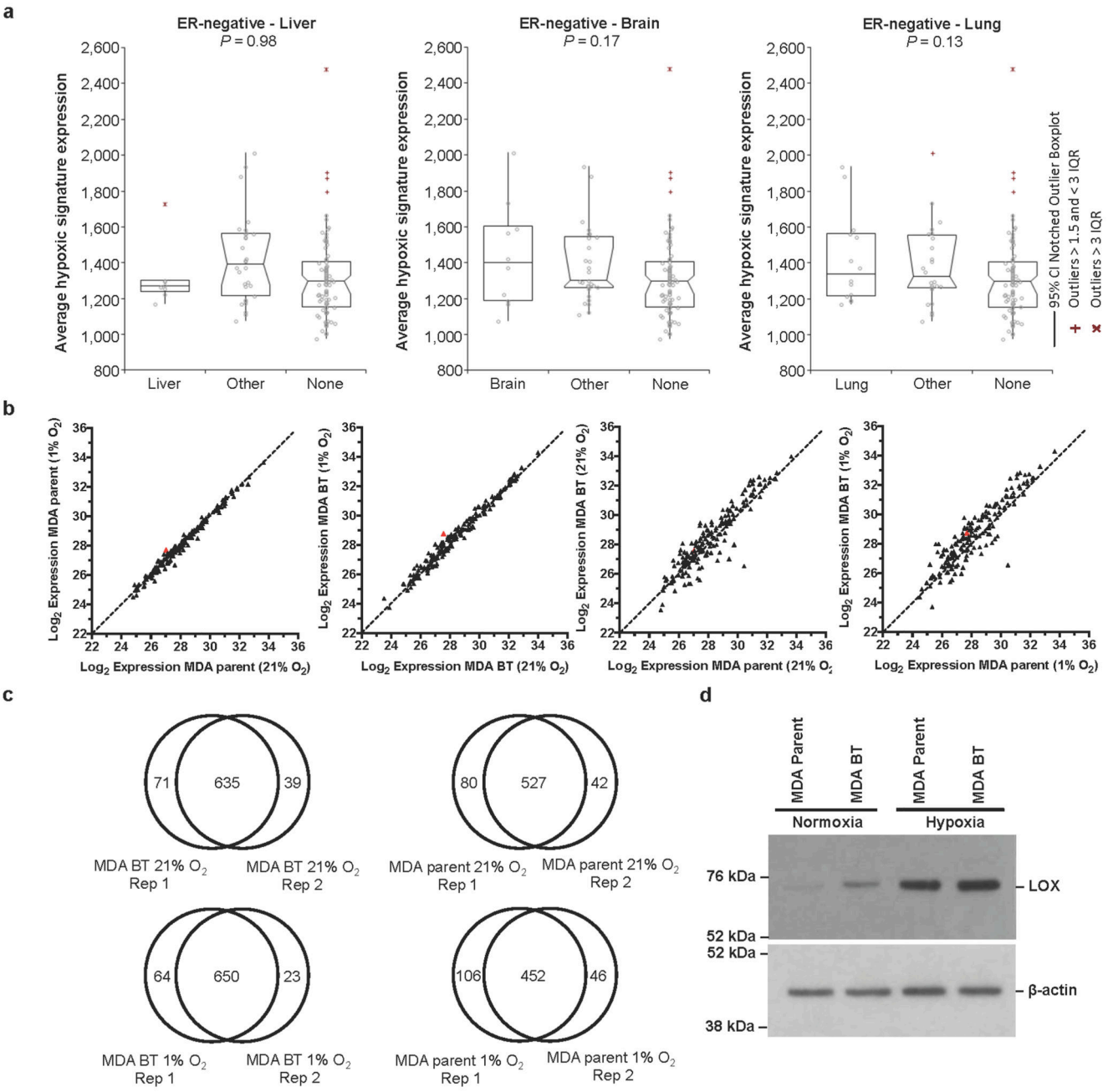

Extended Data Figure 1. LOX is hypoxia regulated and strongly associated with osteotropism and metastasis.

a, Retrospective analysis of our patient cohort including only ER-negative patients showed that the hypoxic signature is not significantly associated with liver relapse (*P*=0.98), brain relapse (*P*=0.17) or lung relapse (*P*=0.13). **b**, Log_2 expression levels under conditions of hypoxia (1% O2) and normoxia (21% O2) for secreted proteins from the MDA-MB-231 parent and MDA-MB-231 Bone Tropic (BT) 1833 cell line. Data representative of 4 repeats,

Europe PMC Funders Author Manuscripts

2x label-free repeats, and 2x SILAC (standard and reverse-label) repeats. Acquisition performed on the Orbitrap Q-Exactive (Thermo Fisher Scientific). **c**, Overlaps between repeats of global secretome analysis in MDA-MB-231 parent and MDA-MB-231 Bone Tropic (BT) cells grown in normoxic (21% O2) and hypoxic (1% O2) conditions from label-free and SILAC approaches. **d**, Immunoblotting for LOX in MDA parent and 1833 Bone Tropic (BT) subclone under conditions of hypoxia (1% O2) and normoxia (21% O2) confirming expression levels seen in proteomic and transcriptomic analyses. Scans of original western blots available as Supplementary Information.

a

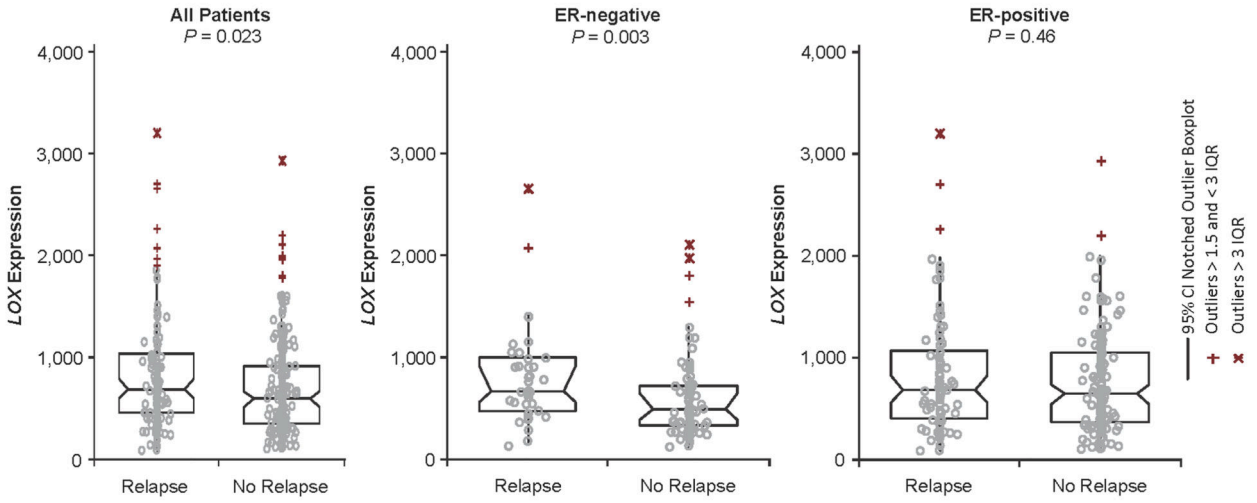

b

Group - All patients n = 344

LOX by Site	n	Rank sum	Mean rank
Bone Relapse	71	14004.0	197.24
Elsewhere Relapse	47	8349.0	177.64
No Relapse	226	36987.0	163.66

Kruskal-Wallis' statistic	6.31	
X^2 statistic	6.31	
DF	2	
p	0.0427	(chisqr approximation, corrected for ties)

Bonferroni Contrast	Difference	*p*
Bone vs. Elsewhere	19.6011	0.8768
Bone vs. No	33.5801	**0.0389**
Elsewhere vs. No	13.9790	1.0000

Group - ER-neg n = 123

LOX by Site	n	Rank sum	Mean rank
Bone Relapse	10	891.0	89.10
Elsewhere Relapse	28	2009.0	71.75
No Relapse	85	4726.0	55.60

Kruskal-Wallis' statistic	10.61	
X^2 statistic	10.61	
DF	2	
p	0.0050	(chisqr approximation, corrected for ties)

Bonferroni Contrast	Difference	*p*
Bone vs. Elsewhere	17.3500	0.5187
Bone vs. No	33.5000	**0.0126**
Elsewhere vs. No	16.1500	0.0988

Group – ER-pos n = 221

LOX by Site	n	Rank sum	Mean rank
Bone Relapse	61	7223.0	118.41
Elsewhere Relapse	19	1998.0	105.16
No Relapse	141	15310.0	108.58

Kruskal-Wallis' statistic	1.18	
X^2 statistic	1.18	
DF	2	
p	0.5545	(chisqr approximation, corrected for ties)

Bonferroni Contrast	Difference	*p*
Bone vs. Elsewhere	13.2519	1.0000
Bone vs. No	9.8283	0.9537
Elsewhere vs. No	-3.4237	1.0000

c

LOX	Group	Hazard Ratio (HR)	*p*-value	95% Conf. Int.
Relapse vs. No relapse	ALL	1.25	0.022	1.03 - 1.51
	ER-NEG	1.6	0.013	1.11 - 2.31
	ER-POS	1.12	0.322	0.90 - 1.39
Bone relapse vs. No relapse	ALL	1.37	0.015	1.06 - 1.76
	ER-NEG	2.55	0.014	1.21 - 5.39
	ER-POS	1.17	0.240	0.90 - 1.51

Extended Data Figure 2. Extended patient data analysis.

a, Across all breast cancer patients, the expression of *LOX* is associated with metastasis formation (*P*=0.023) and in particular with ER-Negative breast cancer patients *(P*=0.0029).

b, An additional Kruskall-Wallis test between reported bone relapse, relapse elsewhere and no relapse patients with an additional contrast test wherein all pairwise groups were considered shows that in all patients, *LOX* expression is associated with bone relapse compared to no relapse (P=0.0389). This also pertains to ER-negative patients (P=0.0126) but not ER-positive patients (P=0.9537). **c**, Cox-regression using $\log_2$-LOX expression data was used to estimate the Hazard Ratio (HR) in two analyses. One analysis was performed using the no-relapse patients and the bone relapse patients (data belonging to Fig.1f) and the second analysis including all patients (data belonging to Extended Data Fig.2a). *LOX* expression is associated with increased Hazard Ratio particularly in ER-negative patients in both analyses.

Europe PMC Funders Author Manuscripts

Europe PMC Funders Author Manuscripts

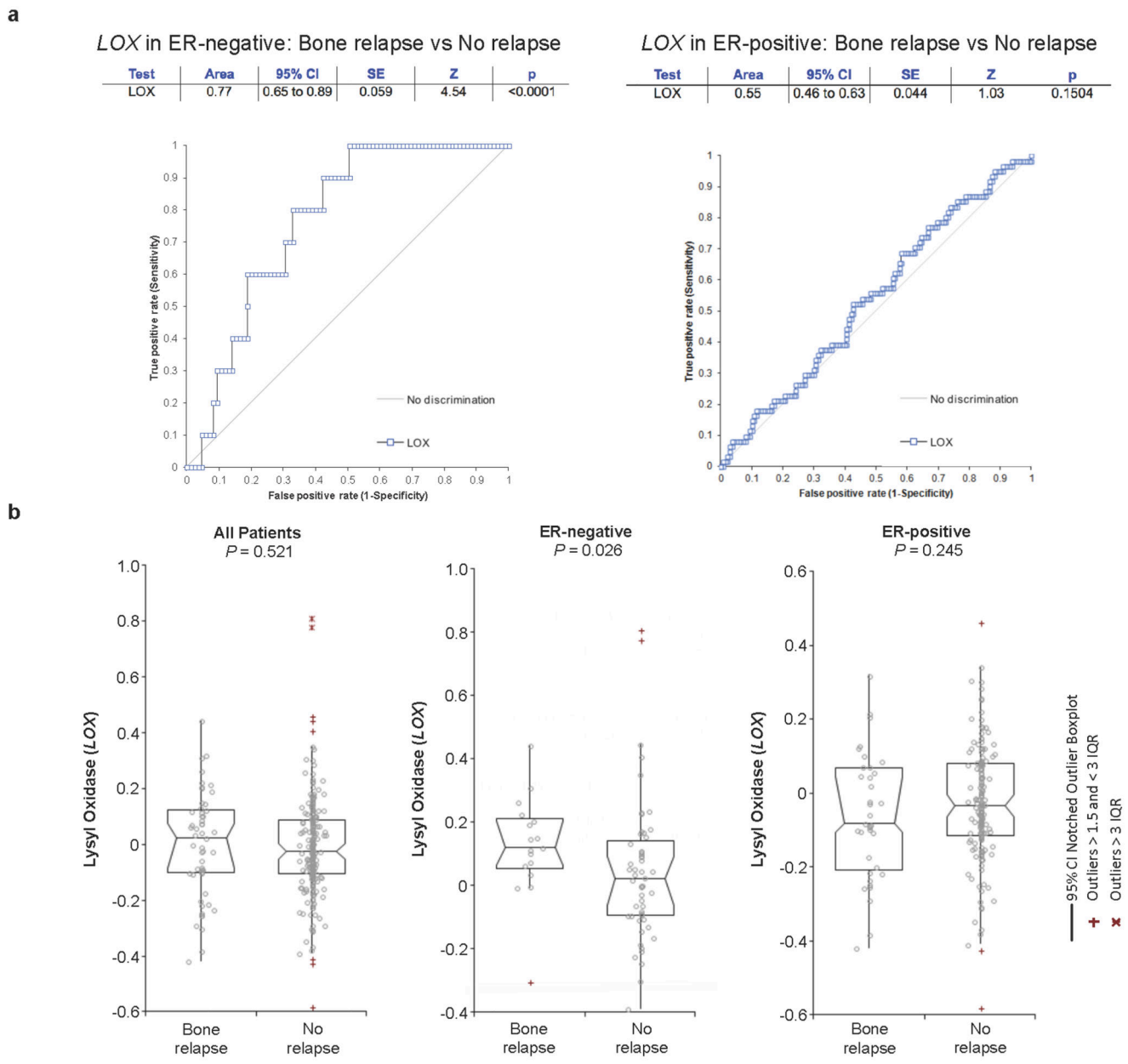

Extended Data Figure 3. Additional patient data analysis in a supporting patient cohort.

a, ROC curve analysis shows *LOX* expression may be indicative of metastatic dissemination of ER-negative breast cancer (AUC 0.77, $P<0.0001$) but not ER-positive patients (AUC 0.55, $P<0.1504$). **b**, In an alternative second patient dataset (Van de Vijver et al. [pubmed ID: 12490681]) reporting data on 295 lymph node negative (LNN) patients who did not receive adjuvant therapy, with available site of relapse, *LOX* is significantly higher expressed in bone relapse ER-negative patients, compared to other groups confirming data from the original dataset.

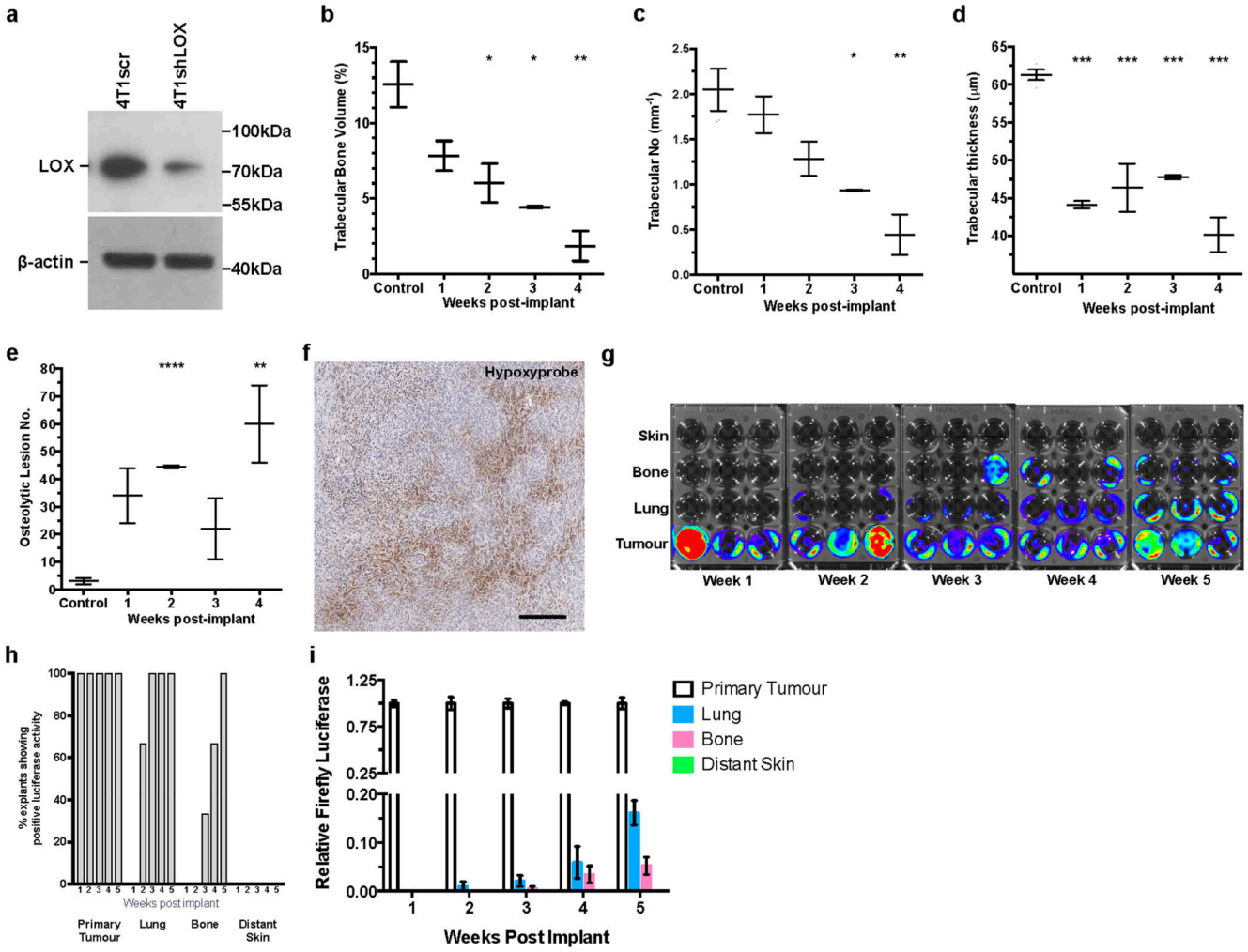

Extended Data Figure 4. Hypoxia-induced tumour-derived LOX stimulates osteolytic lesion formation in the absence of tumour cells.

a, Immunoblotting of 4T1 mammary carcinoma line stably expressing either a scrambled (scr) or shLOX vector which leads to a significant decrease in levels of detectable LOX. Scans of original western blots available as Supplementary Information. **b**, Micro-CT scanning and reconstruction with structural analysis shows decreases in trabecular bone volume (as a percentage of total bone volume) (n=3 mice per group). **c**, decreases in trabecular number (per mm) (n=3 mice per group) and **d**, decreases in trabecular thickness in tibiae of mice bearing 4T1scr mammary fatpad tumours over time (n=3 mice per group). **e**, Micro-CT analysis of mouse tibiae shows increases in focal osteolytic lesions in 4T1scr tumour bearing mice develop over time (n=3 mice per group). (a-e) *P*-values derived from unpaired parametric two-tailed t-test (**P*<0.05**, *P*<0.01, ****P*<0.001). **f**, Representative immunohistochemical staining for pimonidazole (Hypoxyprobe) in 4μm section of 4T1 orthotopic mammary carcinoma, 3 weeks post-implantation shows hypoxia (brown staining) as a salient feature of tumours. Scale bar = 250μm. **g**, Bioluminescent imaging of luciferase signal 2 weeks post explant of samples taken from primary tumour, lung, bone marrow (femur and tibia) and distant skin samples at 1 – 5 weeks post primary tumour implant.

Europe PMC Funders Author Manuscripts

Selection was under 500ug/mL zeocin for the Luciferase expression cassette (n=3 mice per timepoint). **h**, Quantification of (g) as a percentage of positive luciferase expressing explants from various sites following 4T1 tumour implant shows tumour cells do not begin to arrive in the bone until 3 weeks. **i**, Q-RTPCR detection of luciferase expressing 4T1 tumour cells in secondary organs confirms explant culture experiments (n=3 mice per timepoint).

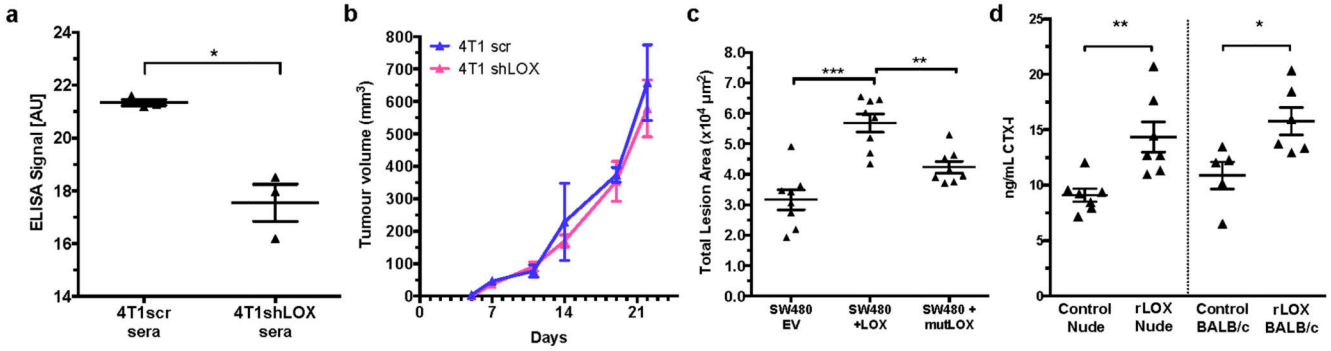

Extended Data Figure 5. Effects of LOX modulation on circulating sera levels, primary tumour growth and osteolytic lesion formation.

a, Enzyme-linked immunosorbent assay (ELISA) for LOX in the sera of 4T1scr and 4T1shLOX tumour bearing mice (n: ELISA signal [AU] in mouse sera: 3 mice per group) shows decreased levels of circulating LOX upon genetic silencing at the primary tumour. Data shown is mean ± SEM. *P*-values derived from unpaired parametric two-tailed t-test (**P*<0.05). **b**, Growth curves as determined by calliper measurement for orthotopic 4T1scr and 4T1shLOX mammary tumours show no difference between primary tumour growth (n: mice; 3 per group). **c**, Injection of hypoxic CMs from SW480 human colorectal cancer cells stably expressing one of; empty vector control (EV), full-length LOX (+LOX), or a catalytically inactive full-length LOX (+mutLOX)(K320A) confirms a LOX-dependent mechanism of focal osteolytic lesion generation in a second human model of cancer. (n: mice; 8 per group). Data shown is mean ± SEM. *P*-values derived from unpaired parametric two-tailed t-test (***P*<0.01, ****P*<0.001). **d**, C-terminal telopeptide (CTX) ELISA (Ratlaps) on sera of mice injected intraperitoneally biweekly with rLOX for 3 weeks. CTX is a telopeptide that can be used as a biomarker in the serum to measure the rate of bone turnover (n: ng/mL circulating CTX-I in mouse sera; 5 mice per group). Data shown is mean ± SEM. *P*-values derived from unpaired parametric two-tailed t-test (**P*<0.05, ***P*<0.01, ****P*<0.001).

Europe PMC Funders Author Manuscripts

Europe PMC Funders Author Manuscripts

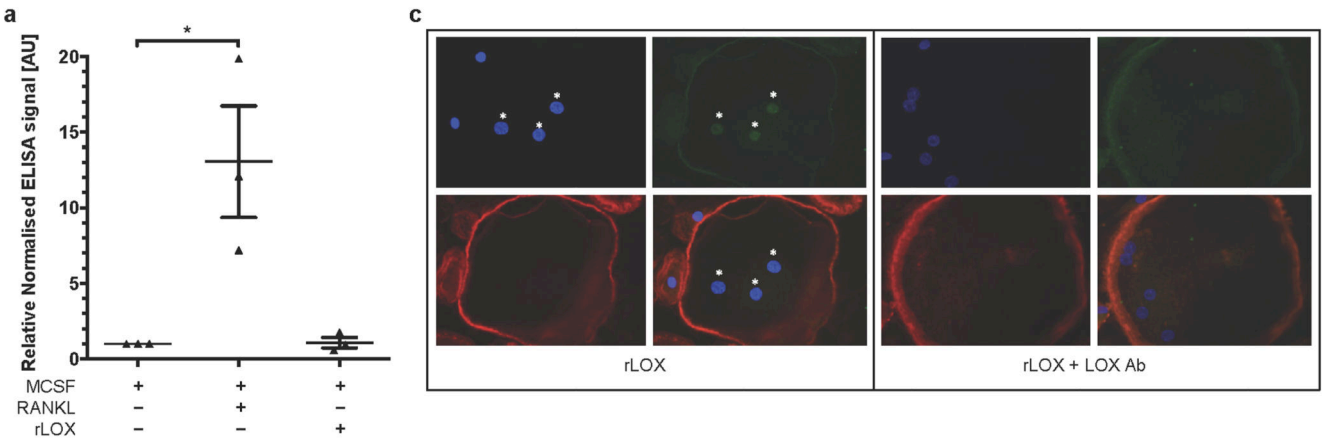

b

Ensembl ID	Gene Name	Description	Unique pep	Mol. weight [kDa]	Seq length	PEP	Intensity	Contaminant
P02769 SWISS-PR	ALB	P02769 (ALBU_BOVIN) (Bos taurus) Bovine serum albumin	9	69.293	607	0.00E+00	151570000	+
P28300 SWISS-PR	**LOX**	**P28300 (LYOX_HUMAN) (Homo sapiens) Lysyl oxidase**	**4**	**46.944**	**417**	**4.19E-52**	**18521000**	
Q3MHN5 SWISS-PR	GC	Q3MHN5 (VTDB_BOVIN) (Bos taurus) Vitamin D-binding protein precursor	2	53.661	475	9.89E-53	33627000	+
P04264 SWISS-PR	KRT1	P04264 (K2C1_HUMAN) (Homo sapiens) Keratin, type II cytoskeletal 1	2	66.017	644	5.80E-84	17794000	+

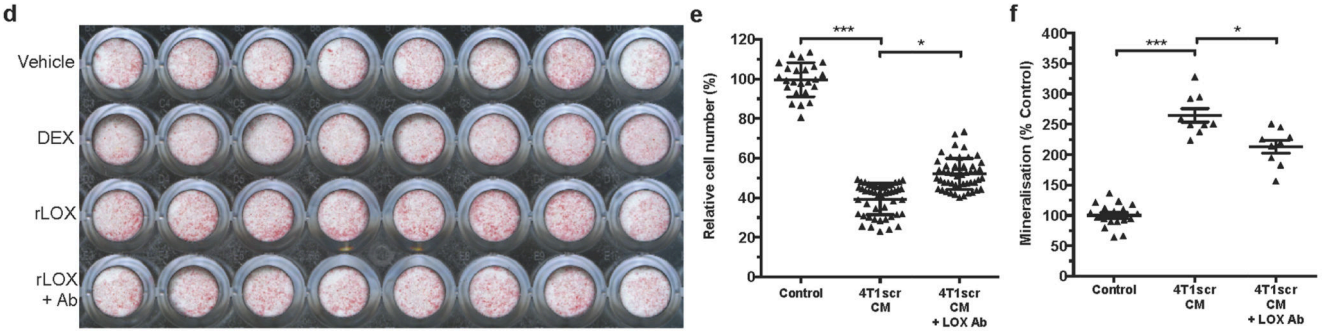

Extended Data Figure 6. LOX modulates osteoclasts and osteoblast behaviour independent of RANKL.

a, ELISA for RANKL in the conditioned media (CM) of osteoclast cultures shows no detectable levels of RANKL in MCSF alone (-ve control) and rLOX cultures excluding the likelihood of autocrine production by cells in response to rLOX (n: ELISA signal [AU]; data is from 3x independent experimental repeats in all groups). Data shown is mean ± SEM. *P*-values derived from unpaired parametric two-tailed t-test. (**P*<0.05) **b**, All proteins detected by Mass Spectrometry analysis in the rLOX preparations (based on MaxQuant 1.5 peptide ID score of 50 and a minimum of 2 unique MS peptide observations). **c**, Examples of nuclear localisation of NFATc1 following addition of rLOX in the presence and absence of the LOX antibody; Green – NFATc1, Red - Phalloidin , Blue – DAPI). **d**, Representative Alizarin Red S plate showing mineralisation ability (calcium deposits as detected by Alizarin Red S staining) of primary calvarial mouse osteoblasts following treatment with dexamethasone (DEX) (positive control) or rLOX ± LOX ab; quantification shown in Fig.3g **e**, High LOX containing hypoxic 4T1scr CM significantly reduces cell proliferation of the human osteoblast like SaOS-2 cell line which can be partially blocked by treatment with anti-LOX antibody (n: normalised cell number per well; control 24 wells; 4T1scr CM 49 wells; 4T1scr CM + LOX Ab 51 wells). Data collected over 3 independent experimental repeats. Data shown in mean ± SEM. *P*-values derived from unpaired parametric two-tailed t-test. (**P*<0.05, ***P*<0.01, ****P*<0.001). **f**, Mineralisation ability (calcium deposits as

detected by Alizarin Red S staining) is increased in the human osteoblast like SaOS-2 cell line in response to high LOX expressing hypoxic 4T1scr CM, the effects of which can be attenuated using the anti-LOX antibody. (n: Alizarin Red S staining per well, data taken from 3 independent repeats; control 18 wells; 4T1scr CM 9 wells; 4T1scr CM + LOX Ab 9 wells). Data shown is mean ± SEM. *P*-values derived from unpaired parametric two-tailed t-test. (**P*<0.05, ***P*<0.01, ****P*<0.001).

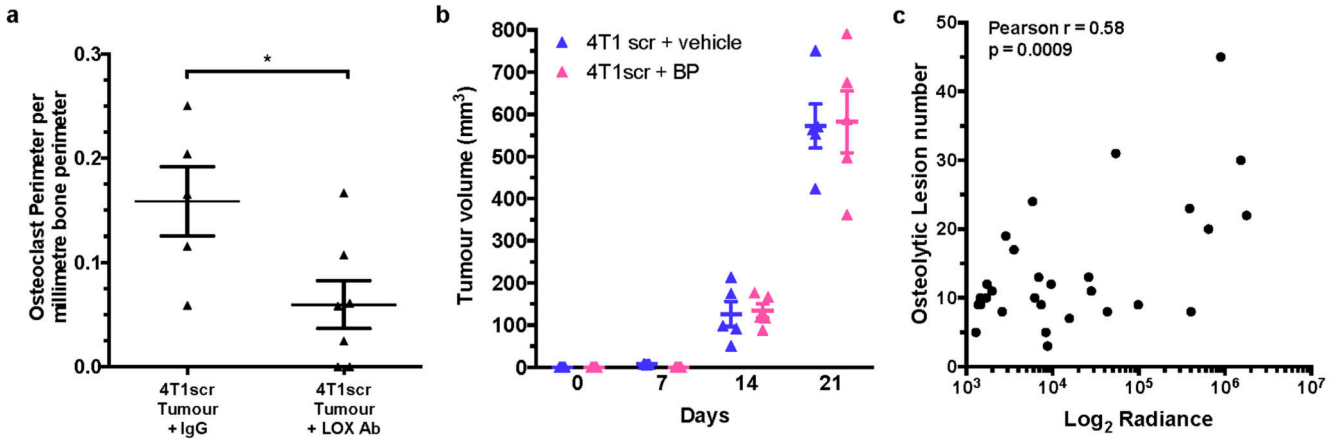

Extended Data Figure 7. Additional *in vivo* analysis of lesion formation and primary tumour growth.

a, 4T1scr tumour bearing mice treated with our LOX antibody show a decrease in osteoclast perimeter in tibial bones in support of LOX as a modulator of osteoclastogenesis shown in Fig.3 (n: mice; 4T1scr Tumour + IgG 5, 4T1scr Tumour + LOX Ab 7). Data shown is mean ± SEM. *P*-values derived from unpaired parametric two-tailed t-test. (**P*<0.05) **b**, Weekly tumour volumetric measurements for 4T1scr tumour bearing mice treated with either zoledronic acid (0.6mg/kg intraperitoneally) or vehicle (PBS), show that when administered alone zoledronic acid does not affect primary 4T1scr primary tumour growth *in vivo* (n: mice; 4 in all groups). **c**, Pearson correlation shows a moderate correlation between lesion number as determined by micro-CT analysis and luciferase signal (radiance [p/s/cm^2/sr]) from 4T1Luc tumour cells within the bone (r = 0.58, 95% CI 0.2778 – 0.7834, *P* = 0.0009 [two-tailed]).

Supplementary Material

Refer to Web version on PubMed Central for supplementary material.

Acknowledgements

We thank the animal welfare staff at the Institute of Cancer Research and Biocentre (University of Copenhagen); the Bone Analysis Laboratory (The University of Sheffield); M. Smid, J. W. M. Martens and J. A. Foekens (Erasmus MC Cancer Institute, Rotterdam, The Netherlands) for in-depth patient data analyses; and A. J. Giaccia and members of our laboratories for comments. This research was supported by funding from Cancer Research UK (C107/A10433) (T.R.C., D.B., G.L.J.T.E.), the Biotech Research and Innovation Centre (BRIC, University of Copenhagen) (T.R.C.), The University of Sheffield (A.G., I.D.H.), National Institute for Health Research Sheffield Clinical Research Facility (A.G.), Breast Cancer Campaign (#2012MayPR086) (A.G., R.M.H.R.), and the Danish Cancer Society (R56-A2971-12-S2) (A.M.H.). Experiments in the laboratory of R.L. were funded by The Lundbeck Foundation and the work was supported by the Velux Foundations (VKR)-funded Instrument Center for Systems

Proteomics (VKR 022758). L.P. and J.T.E. are supported by a Hallas Møller Stipendum from the Novo Nordisk Foundation.

References

1. Chan DA, Giaccia AJ. Hypoxia, gene expression, and metastasis. Cancer Metastasis Rev. 2007; 26:333–339. [PubMed: 17458506]
2. Jin L, et al. Differential secretome analysis reveals CST6 as a suppressor of breast cancer bone metastasis. Cell Res. 2012; 22:1356–1373. [PubMed: 22688893]
3. Erler JT, et al. Hypoxia-induced lysyl oxidase is a critical mediator of bone marrow cell recruitment to form the premetastatic niche. Cancer Cell. 2009; 15:35–44. [PubMed: 19111879]
4. Kaplan RN, et al. VEGFR1-positive haematopoietic bone marrow progenitors initiate the pre-metastatic niche. Nature. 2005; 438:820–827. [PubMed: 16341007]
5. Blanco MA, et al. Global secretome analysis identifies novel mediators of bone metastasis. Cell Res. 2012; 22:1339–1355. [PubMed: 22688892]
6. Coleman RE, Rubens RD. The clinical course of bone metastases from breast cancer. British journal of cancer. 1987; 55:61–66. [PubMed: 3814476]
7. Steeg PS. Tumor metastasis: mechanistic insights and clinical challenges. Nat Med. 2006; 12:895–904. [PubMed: 16892035]
8. Chi JT, et al. Gene Expression Programs in Response to Hypoxia: Cell Type Specificity and Prognostic Significance in Human Cancers. PLoS Med. 2006; 3:e47. [PubMed: 16417408]
9. Smid M, et al. Subtypes of breast cancer show preferential site of relapse. Cancer Research. 2008; 68:3108–3114. [PubMed: 18451135]
10. Kang Y, et al. A multigenic program mediating breast cancer metastasis to bone. Cancer Cell. 2003; 3:537–549. [PubMed: 12842083]
11. El-Haibi CP, et al. Critical role for lysyl oxidase in mesenchymal stem cell-driven breast cancer malignancy. Proc Natl Acad Sci U S A. 2012; 109:17460–17465. [PubMed: 23033492]
12. Cox TR, et al. LOX-mediated collagen crosslinking is responsible for fibrosis-enhanced metastasis. Cancer Research. 2013; 73:1721–1732. [PubMed: 23345161]
13. Erler JT, et al. Lysyl oxidase is essential for hypoxia-induced metastasis. Nature. 2006; 440:1222–1226. [PubMed: 16642001]
14. van de Vijver MJ, et al. A gene-expression signature as a predictor of survival in breast cancer. N Engl J Med. 2002; 347:1999–2009. [PubMed: 12490681]
15. Baker AM, Bird D, Lang G, Cox TR, Erler JT. Lysyl oxidase enzymatic function increases stiffness to drive colorectal cancer progression through FAK. Oncogene. 2012; 32:1863–1868. [PubMed: 22641216]
16. Boyle WJ, Simonet WS, Lacey DL. Osteoclast differentiation and activation. Nature. 2003; 423:337–342. [PubMed: 12748652]
17. Garrett IR, et al. Oxygen-derived free radicals stimulate osteoclastic bone resorption in rodent bone in vitro and in vivo. The Journal of clinical investigation. 1990; 85:632–639. [PubMed: 2312718]
18. Bax BE, et al. Stimulation of osteoclastic bone resorption by hydrogen peroxide. Biochemical and biophysical research communications. 1992; 183:1153–1158. [PubMed: 1567393]
19. Hiratsuka S, Watanabe A, Aburatani H, Maru Y. Tumour-mediated upregulation of chemoattractants and recruitment of myeloid cells predetermines lung metastasis. Nat Cell Biol. 2006; 8:1369–1375. [PubMed: 17128264]
20. Monteiro AC, et al. T cells induce pre-metastatic osteolytic disease and help bone metastases establishment in a mouse model of metastatic breast cancer. PLoS One. 2013; 8:e68171. [PubMed: 23935856]
21. Barker HE, Cox TR, Erler JT. The rationale for targeting the LOX family in cancer. Nat Rev Cancer. 2012; 19:540–552. [PubMed: 22810810]
22. Vora SR, et al. Lysyl oxidase propeptide inhibits FGF-2-induced signaling and proliferation of osteoblasts. The Journal of biological chemistry. 2010; 285:7384–7393. [PubMed: 20048148]

Europe PMC Funders Author Manuscripts

23. Pischon N, et al. Lysyl oxidase (lox) gene deficiency affects osteoblastic phenotype. Calcif Tissue Int. 2009; 85:119–126. [PubMed: 19458888]

24. Feres-Filho EJ, Choi YJ, Han X, Takala TE, Trackman PC. Pre- and post-translational regulation of lysyl oxidase by transforming growth factor-beta 1 in osteoblastic MC3T3-E1 cells. The Journal of biological chemistry. 1995; 270:30797–30803. [PubMed: 8530522]

25. Bondareva A, et al. The lysyl oxidase inhibitor, beta-aminopropionitrile, diminishes the metastatic colonization potential of circulating breast cancer cells. PLoS One. 2009; 4:e5620. [PubMed: 19440335]

26. Wang N, et al. Reduced bone turnover in mice lacking the P2Y(13) receptor of ADP. Mol Endocrinol. 2012; 26:142–152. [PubMed: 22108801]

27. Parfitt AM, et al. Bone histomorphometry: standardization of nomenclature, symbols, and units. Report of the ASBMR Histomorphometry Nomenclature Committee. J Bone Miner Res. 1987; 2:595–610. [PubMed: 3455637]

28. Agrawal, A.; Gallagher, JA.; Gartland, A. Methods in Molecular Biology. Mitry, Ragai R.; Hughes, Robin D., editors. Vol. 806. Humana Press; 2012. p. 357-375.

29. Gartland A, Hipskind RA, Gallagher JA, Bowler WB. Expression of a P2X7 receptor by a subpopulation of human osteoblasts. J Bone Miner Res. 2001; 16:846–856. [PubMed: 11341329]

Europe PMC Funders Author Manuscripts

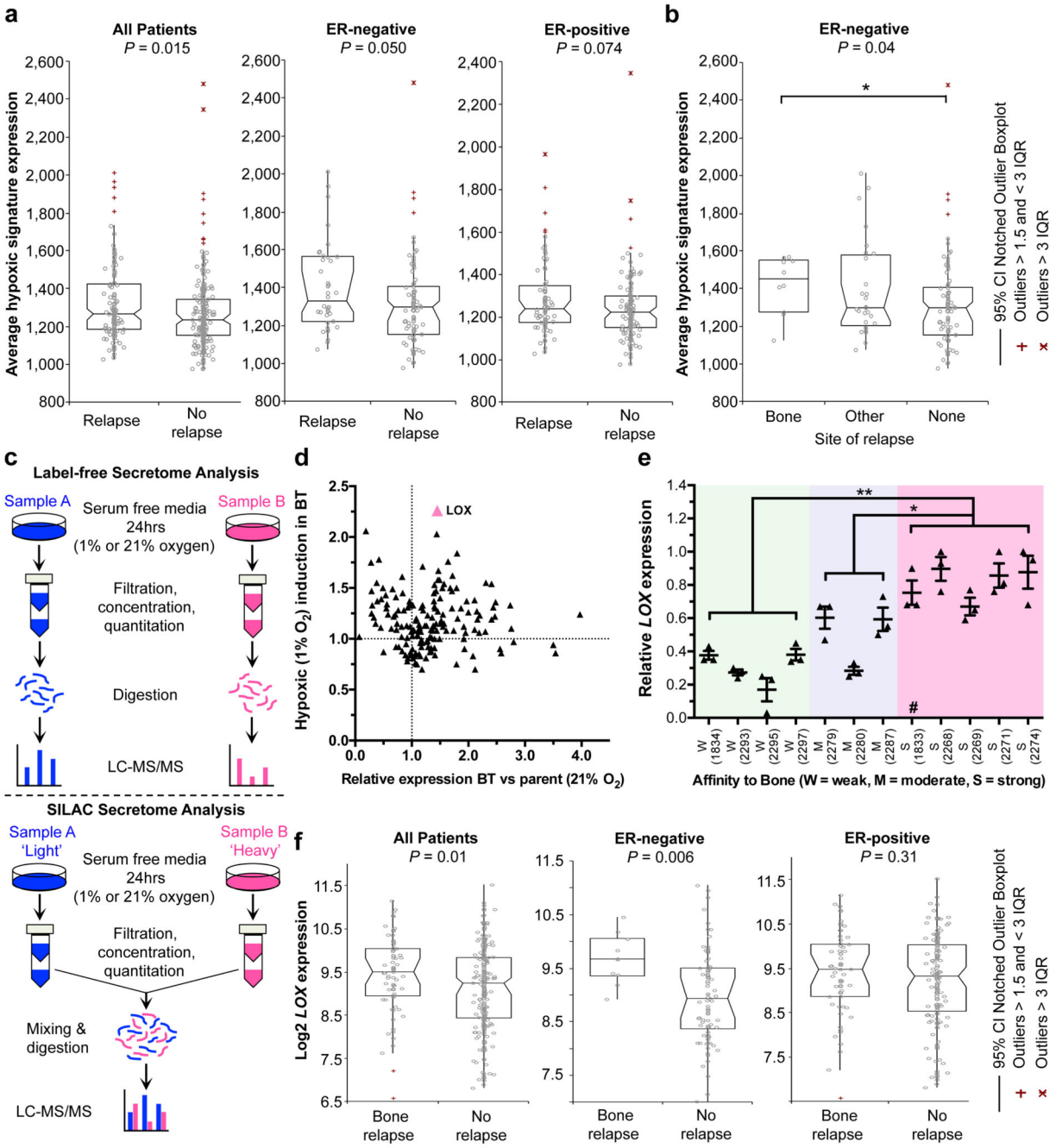

Figure 1. Tumour-secreted LOX is a critical player in ER– breast cancer bone metastasis.

a, Retrospective analysis of 344 LNN primary breast cancers. The hypoxic signature is associated with relapse in all patients, and specifically ER– patients, but not ER+ patients. **b,** Further analysis indicates the hypoxic signature is specifically associated with bone relapse. **c,** Schematic overview of quantitative stable isotope labelling by amino acids in cell culture SILAC and label-free global proteomic secretome analysis approaches. **d,** LOX is more than 1.5 fold upregulated in bone tropic (BT) vs parental cells and the most hypoxia regulated (>2.25 fold) protein associated with osteotropism. A full list is available in Supplementary

Information. **e,** Log_2 median centered expression of *LOX* mRNA in MDA-MB-231 parental and subclone lines (n=3 probesets per cell line) (# indicates 1833 'BT' clone used). *P*-values derived from unpaired parametric two-tailed t-tests (**P*<0.05, ***P*<0.01). **f,** *LOX* expression specifically associates with bone relapse in ER– breast cancer patients but not ER+ patients. (a,b,f) *P*-values derived from a 2-tailed Mann-Whitney test.

Europe PMC Funders Author Manuscripts

Europe PMC Funders Author Manuscripts

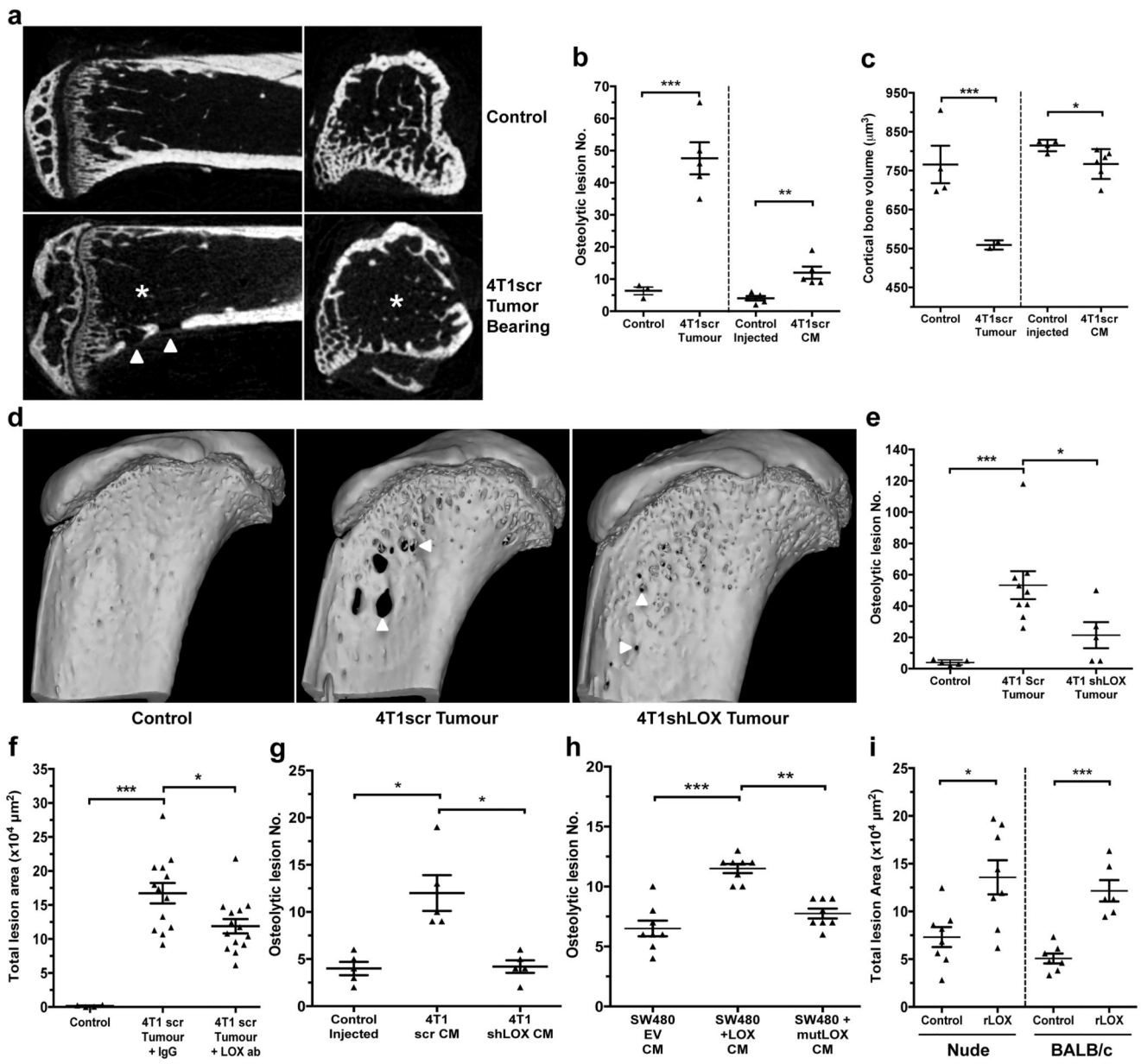

Figure 2. Osteolytic lesion formation in ER– mammary carcinoma models is LOX dependent.

a, Representative 2D cross-sections of tibia from control (top) and tumour-bearing (bottom) mice 3-weeks post orthotopic implantation showing lesions (arrowheads) and loss of trabecular structure (asterisks). **b,** Micro-CT analysis of osteolytic lesions in tumour-bearing and tumour-free, CM conditioned mice at 3 weeks (n: mice; control 3; 4T1scr Tumour 5; Control Injected 5; 4T1scr CM 5) **c,** Loss of cortical bone volume in 4T1scr tumour-bearing and tumour-free CM injected models at 3 weeks (n: mice; control 4; 4T1scr Tumour 3; Control Injected 4; 4T1scr CM 6). **d,** Representative 3D reconstructions of tibiae showing tumour driven osteolytic lesions (arrowheads). **e,** LOX silencing decreases focal osteolytic lesion formation (n: mice; control 5; 4T1scr Tumour 8; 4T1 shLOX Tumour 5). **f,** LOX inhibition decreases osteolytic lesion formation in tumour-bearing models (n: mice; control

5; 4T1scr Tumour + IgG 13; 4T1scr Tumour + LOX Ab 14) and **g,** in tumour-free CM injection models (n: mice; control 5; 4T1scr CM 5; 4T1shLOX CM 5) **h,** SW480 human CRC lines with stably manipulated LOX expression (EV, +LOX or +mutLOX) confirms LOX-dependency (n=8 mice per condition). **i,** Exogenous recombinant LOX (rLOX) drives osteolytic lesion formation in Nude and BALB/c models (n: mice; Nude control 8; Nude rLOX 8; BALB/c control 7; BALB/c rLOX 6). (b,c,e,f,g,h,i) Data shown are mean ± SEM. *P*-values derived from unpaired parametric one-tailed t-tests. (**P*<0.05, ***P*<0.01, ****P*<0.001).

Europe PMC Funders Author Manuscripts

Europe PMC Funders Author Manuscripts

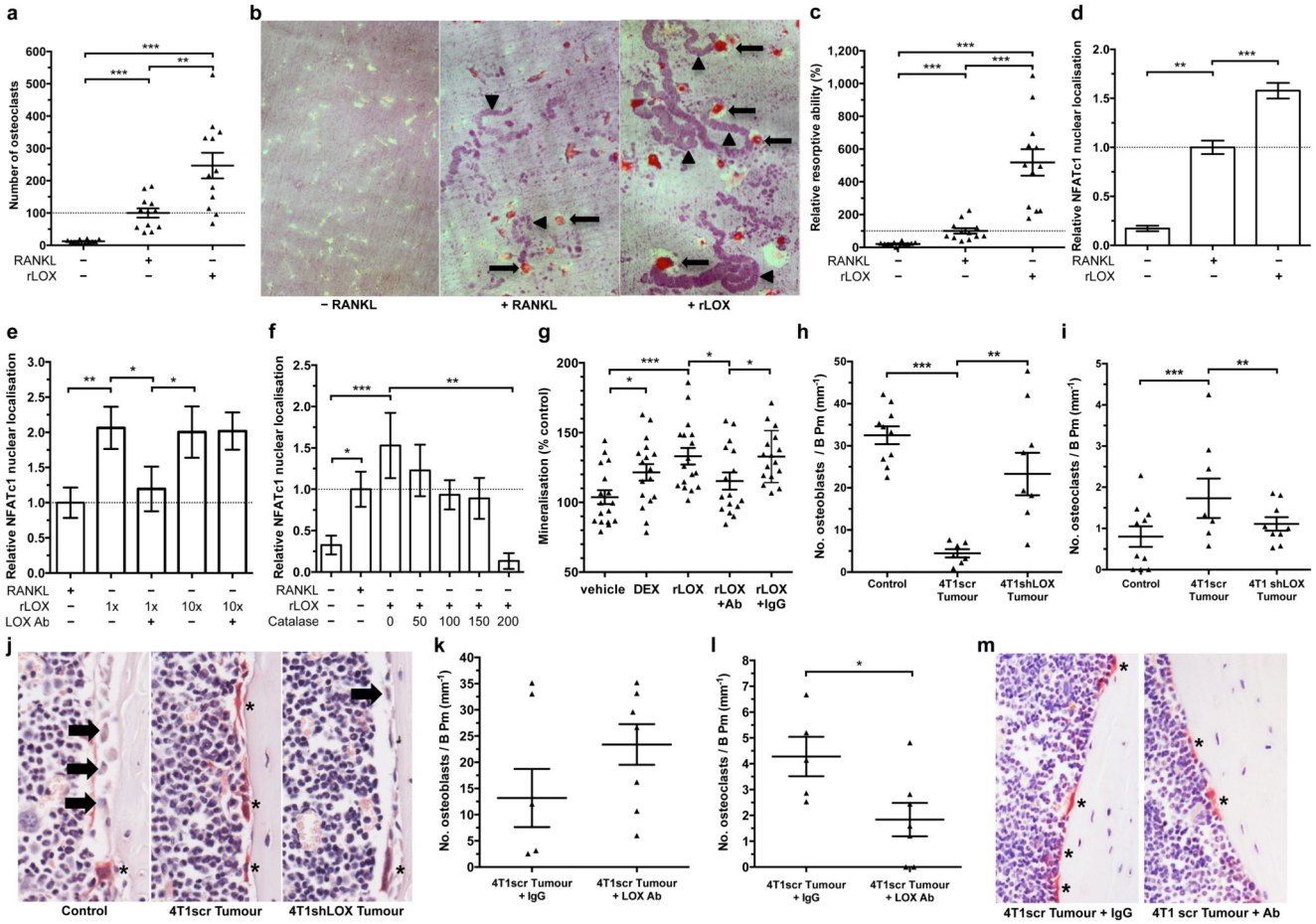

Figure 3. Tumour-secreted LOX modulates osteoclasts and osteoblasts *in vitro* and *in vivo*.

a, rLOX (in the absence of RANKL) stimulates osteoclastogenesis. **b, c,** rLOX generated osteoclasts exhibit high resorptive ability; arrow = osteoclast, arrowheads = resorption tracks. (a-c)(n: osteoclast count from 12 independent osteoclast assays per group). **d,** rLOX induces nuclear localization of the master transcription factor NFATc1 in the absence of RANKL (n: osteoclast NFATc1 nuclear intensity; control 12; +RANKL 196, +rLOX 191 across 3 independent experimental repeats [donors] from 16 fields of view per donor). **e,** LOX antibody treatment blocks NFATc1 localization. **f,** Catalase treatment blocks rLOX-induced nuclear localization of NFATc1 (e,f represents data from 32 measurements of NFATc1 nuclear intensity from each of 3 independent donors [96 total]) **g,** rLOX added to primary mouse calvarial osteoblasts increases mineralization ability (DEX = dexamethasone) (n: alizarin red S intensity; 16 wells per group across 2 independent experimental repeats) **h**, 4T1scr mammary tumours decrease osteoblast number compared to shLOX (n: mice; Control 10; 4T1scr Tumour 7; 4T1 shLOX Tumour 9) and **i,** increase osteoclast number on the endocortical surface of bone (per mm bone perimeter)(n: mice; Control 10; 4T1scr Tumour 8; 4T1 shLOX Tumour 9). **j,** Representative images of osteoblasts (arrows) and osteoclasts (*) in sections of bone. **k,** 4T1scr tumour bearing mice treated with the anti-LOX antibody show similar effects on osteoblast **l,** osteoclast number (n: mice; 4T1scr Tumour + IgG 5; 4T1scr Tumour + LOX Ab 7). **m**, Representative sections

of bone from 4T1scr tumour bearing mice with or without anti-LOX antibody or IgG control). (a,c-i,k,l) Data shown is mean ± SEM. *P*-values derived from unpaired parametric two-tailed t-tests. (**P*<0.05, ***P*<0.01, ****P*<0.001).

Europe PMC Funders Author Manuscripts

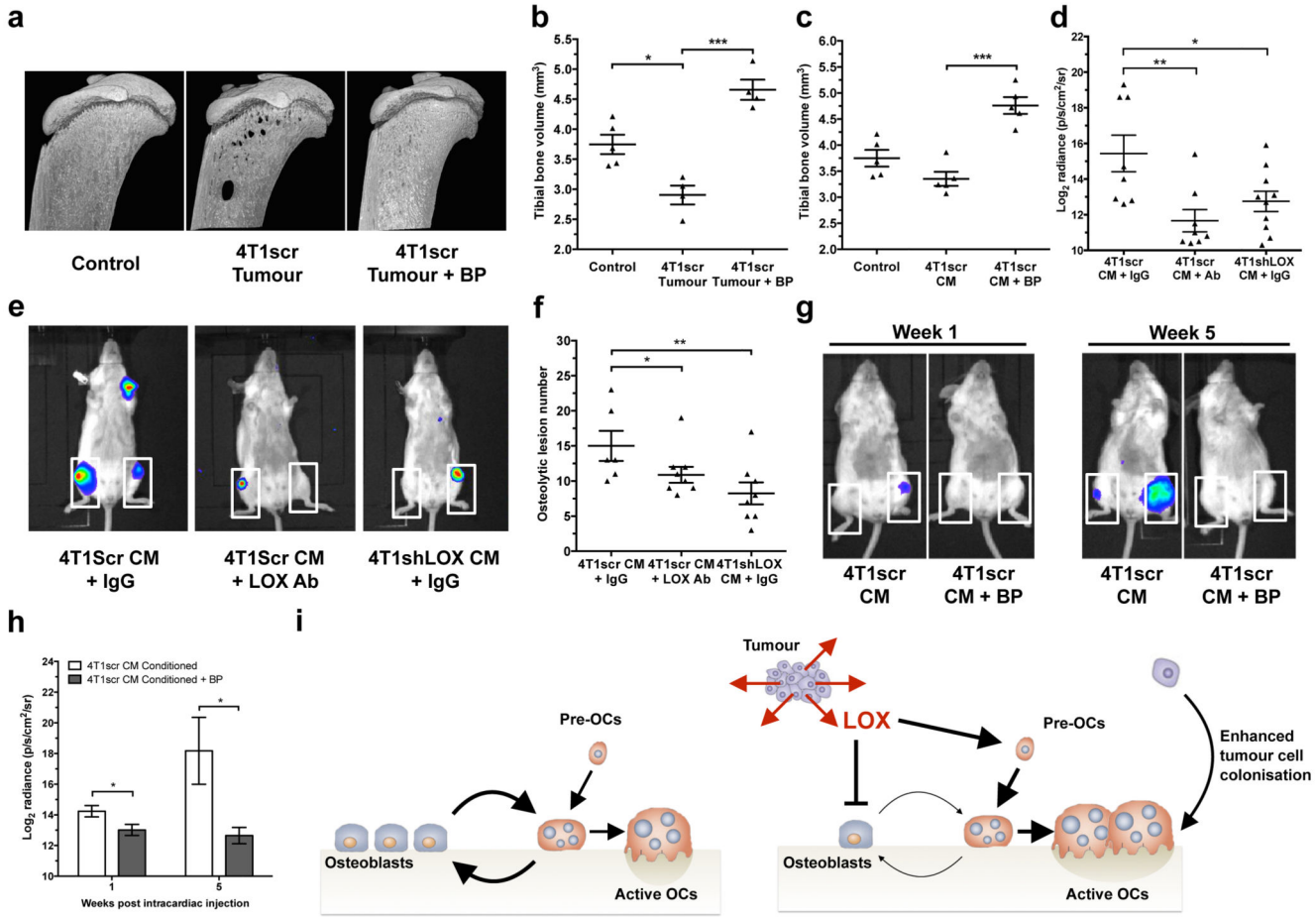

Figure 4. LOX-mediated lesions are osteoclast-driven and enhance circulating tumour cell colonisation.

a, Representative 3D reconstructions of tibiae from tumour bearing mice with or without BP treatment **b**, Tibial bone loss is abrogated in tumour bearing mice treated with bisphosphonate (n: mice; Control 5; 4T1scr Tumour 4; 4T1scr Tumour + BP 4) **c,** Similar effects are observed in CM conditioned models treated with bisphosphonates (n=5 mice all groups) **d**, Quantification of **e**, Whole body IVIS imaging of intracardially injected 4T1Luc tumour cells following conditioning with 4T1scr or 4T1shLOX CM. White boxes – tumour burden analysis region of interest (n: mice; 4T1scr CM+IgG 8; 4T1scr CM+LOXAb 8; 4T1shLOX CM+IgG 10) **f**, Micro-CT lesion analysis of mice after intracardiac injection following pre-conditioning (n: mice; 4T1scr CM+IgG 6; 4T1scr CM+LOXAb 8; 4T1shLOX CM+IgG 8) **g**, Representative whole body IVIS imaging of 4T1Luc tumour cells at 1 week and 5 weeks after intracardiac injection. Mice were conditioned with hypoxic 4T1scr CM with and without simultaneous treatment with bisphosphonate. White boxes – tumour burden analysis region of interest. **h**, Log_2 quantitation of (g) (n=5 mice all groups) **i**, Schematic of LOX mediated effects on bone homeostasis *in vivo.* (b-d,f,h) Data shown is mean ± SEM. *P*-values derived from unpaired parametric two-tailed t-tests. (**P*<0.05, ***P*<0.01, ****P*<0.001).

Europe PMC Funders Author Manuscripts